



# Prediction of tumor response via a pretreatment MRI radiomics-based nomogram in HCC treated with TACE

Chunli Kong<sup>1,2</sup> · Zhongwei Zhao<sup>1,2</sup> · Weiyue Chen<sup>1,2</sup> · Xiuling Lv<sup>1,2</sup> · Gaofeng Shu<sup>1,2</sup> · Miaoqing Ye<sup>1,2</sup> · Jingjing Song<sup>1,2</sup> · Xihui Ying<sup>1,2</sup> · Qiaoyou Weng<sup>1,2</sup> · Wei Weng<sup>1,2</sup> · Shiji Fang<sup>1,2</sup> · Minjiang Chen<sup>1,2</sup> · Jianfei Tu<sup>1,2</sup> · Jiansong Ji<sup>1,2</sup>

Received: 4 September 2020 / Revised: 23 February 2021 / Accepted: 18 March 2021 / Published online: 16 April 2021

© The Author(s) 2021, corrected publication 2021

## Abstract

**Objectives** To develop and validate a pre-transcatheter arterial chemoembolization (TACE) MRI-based radiomics model for predicting tumor response in intermediate-advanced hepatocellular carcinoma (HCC) patients.

**Materials** Ninety-nine intermediate-advanced HCC patients (69 for training, 30 for validation) treated with TACE were enrolled. MRI examinations were performed before TACE, and the efficacy was evaluated according to the mRECIST criterion 3 months after TACE. A total of 396 radiomics features were extracted from T2-weighted pre-TACE images, and least absolute shrinkage and selection operator (LASSO) regression was applied to feature selection and model construction. The performance of the model was evaluated by receiver operating characteristic (ROC) curves, calibration curves, and decision curves.

**Results** The AFP value, Child-Pugh score, and BCLC stage showed a significant difference between the TACE response (TR) and non-TACE response (nTR) patients. Six radiomics features were selected by LASSO and the radiomics score (Rad-score) was calculated as the sum of each feature multiplied by the non-zero coefficient from LASSO. The AUCs of the ROC curve based on Rad-score were 0.812 and 0.866 in the training and validation cohorts, respectively. To improve the diagnostic efficiency, the Rad-score was further integrated with the above clinical indicators to form a novel predictive nomogram. Results suggested that the AUC increased to 0.861 and 0.884 in the training and validation cohorts, respectively. Decision curve analysis showed that the radiomics nomogram was clinically useful.

**Conclusion** The radiomics and clinical indicator-based predictive nomogram can well predict TR in intermediate-advanced HCC and can further be applied for auxiliary diagnosis of clinical prognosis.

## Key Points

- *The therapeutic outcome of TACE varies greatly even for patients with the same clinicopathologic features.*
- *Radiomics showed excellent performance in predicting the TACE response.*
- *Decision curves demonstrated that the novel predictive model based on the radiomics signature and clinical indicators has great clinical utility.*

**Keywords** Therapeutic chemoembolization · Hepatocellular carcinoma · Prognosis · Nomogram

Chunli Kong and Zhongwei Zhao contributed equally to this work.

✉ Jianfei Tu  
jianfei1133@163.com

✉ Jiansong Ji  
jjiansong@zju.edu.cn

<sup>1</sup> Key Laboratory of Imaging Diagnosis and Minimally Invasive Intervention Research, Lishui Hospital of Zhejiang University/the Fifth Affiliated Hospital of Wenzhou Medical University, Lishui 323000, China

<sup>2</sup> Department of Radiology, Affiliated Lishui Hospital of Zhejiang University/the Fifth Affiliated Hospital of Wenzhou Medical University/The Central Hospital of Zhejiang Lishui, Lishui 323000, China

## Abbreviations

95% CI	95% confidence interval
BCLC	Barcelona Clinic Liver Cancer
GLCM	Gray-level co-occurrence matrix
GLSZM	Gray-level size zone matrix
LASSO	Least absolute shrinkage and selection operator
nTR	Non-TACE response
RLM	Run-length matrix
TR	TACE response

## Introduction

Hepatocellular carcinoma (HCC) is the most frequent primary malignancy of the liver with high lethality, and its incidence is steadily rising worldwide [1, 2]. Hepatocarcinogenesis is a complex biological process with multiple steps, in which genomic changes induce the formation of cellular intermediates by progressively altering the hepatocellular phenotype, thereby evolving into HCC [3]. Hepatectomy and liver transplantation are considered the only two options with potentially curative effects [4]. Unfortunately, most HCC patients are diagnosed at an intermediate-advanced stage with accompany of extensive diseases or underlying liver dysfunction and are often not eligible for curative therapies. According to the Barcelona Clinic Liver Cancer (BCLC) clinical staging system, local therapy represented by transcatheter arterial chemoembolization (TACE) has become an important therapy for patients with intermediate-advanced liver cancer [5].

As a globally used approach for effective treatment of inoperable HCC, TACE also builds a bridge for connection with other therapies, such as hepatectomy [6] and targeted therapy [7]. However, the therapeutic outcome of TACE varies greatly from patient to patient because the biological behavior of tumor cells is highly heterogeneous [8]. Recent studies have evidenced that the heterogeneity of TACE response also results in a high incidence of local tumor recurrence, which could reach to 46%, 58%, and 63% at 2, 3, and 5 years of posttreatment, respectively [9–11]. Previous studies have confirmed that Cezanne and cytokine signaling 3 methylation are highly related to the heterogeneity of TACE response [8, 12]. Although many efforts have been made, reliable methods related to the prediction of the response to TACE treatment and the prognosis of HCC patients are still limited. To revolutionize the treatment of HCC, an accurate and efficient method for the prediction of TACE response is needed, which is also the key goal of modern personalized medicine [13]. Clinically, magnetic resonance imaging (MRI) plays an essential role in the initial staging, therapeutic strategy, and treatment response assessment of HCC [14]. The current MRI-based diagnosis relies on the experience of radiologists, who make a subjective and qualitative interpretation based on the image. However, it is difficult for them to make a quantitative assessment of tumor heterogeneity [15]. Currently, there is a growing interest in the utilization of radiomics for diagnosis, which could characterize the phenotypes of different diseases by extracting quantitative features from medical images. Previous studies have demonstrated that features based on radiomics are inextricably linked to clinical prognosis and underlying genomic patterns across a range of cancer types [16–18]. Therefore, it may be feasible to predict the TACE response by using radiomics, which could well establish the link between HCC and medical images [19]. To our knowledge, MRI-based radiomics is still inadequate for the prediction of TACE response.

Therefore, the aim of this study was to develop and validate an MRI-based radiomics nomogram that could provide individualized pretreatment evaluations of the TACE response of HCC and to assess the feasibility of its clinical application.

## Materials and methods

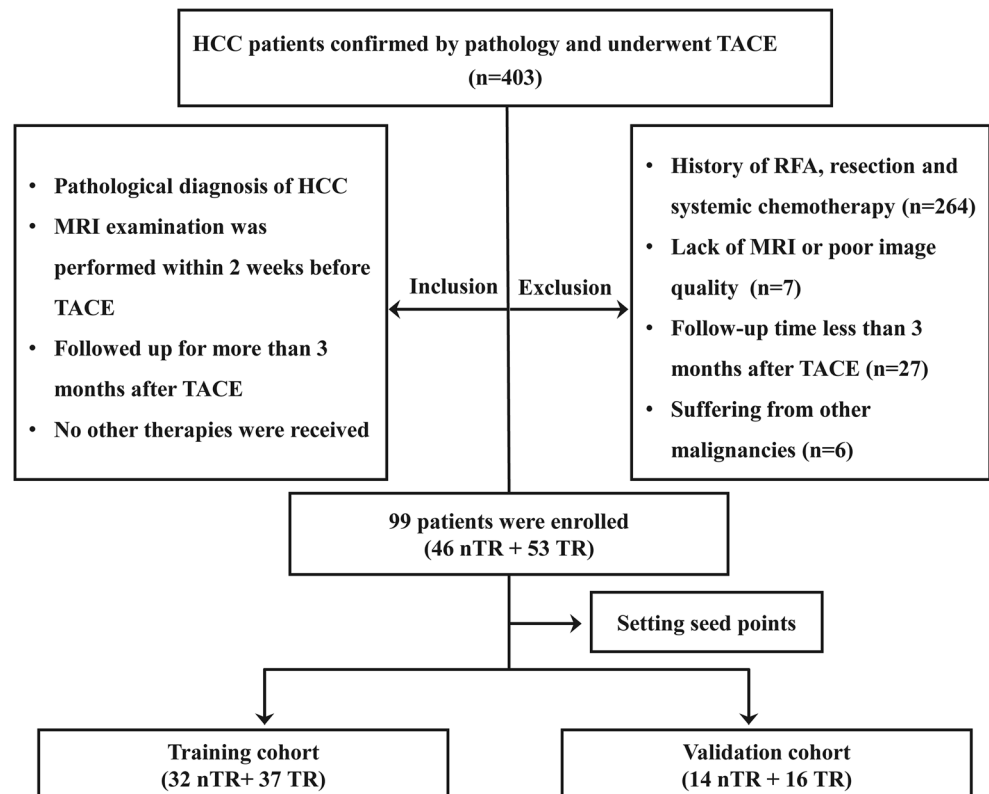
### Patient selection

The study was approved by the Institutional Review Board and Human Ethics Committee of Lishui Hospital of Zhejiang University, and the requirement for informed consent was waived. A total of 403 patients who underwent TACE treatment in our institution with pathologically confirmed intermediate (BCLC stage B) or advanced (BCLC stage C) HCC were enrolled from March 2016 to December 2019. Other inclusion criteria for eligible patients included MRI examination performed within 2 weeks before TACE and follow-up for more than 3 months after TACE, as well as no other therapies. A total of 304 patients were excluded due to the following factors: (1) patients who received a combination of other treatments, such as tumor resection, radiotherapy, or systemic chemotherapy ( $n = 264$ ); (2) patients who lacked MR imaging data or poor image quality ( $n = 7$ ); (3) patients with a follow-up time after TACE of less than 3 months ( $n = 27$ ); and (4) patients with other malignancies ( $n = 6$ ). Finally, 99 patients were selected for further study in the present study. The flow of the case identification process is shown in Fig. 1.

### MR imaging protocol

All MRI scans were performed on a Philips ENGENTIA 3.0-T MR scanner (Philips Medical Systems). All patients underwent dynamic contrast MRI before and after TACE, and corresponding standard clinical protocols included (1) spectral presaturation with inversion recovery T2-weighted sequence (repetition time/echo time (TE), 3000/200 ms; slice thickness, 7 mm; interslice gap, 1 mm; matrix size,  $200 \times 195$ ); (2) breath-hold unenhanced and contrast-enhanced (after injection of 0.1 mmol gadopentetate dimeglumine (Guangzhou Kangchen Pharmaceutical Co. Ltd.) per kilogram of body weight) mDIXON-T1WI (water) sequence (repetition time/TE1/TE2, 3.6/1.31/2.2 ms; field of view, 400–314 mm; slice thickness, 5 mm; slice gap, –2.5 mm; matrix size,  $224 \times 166$ ) were scanned, and 4 dynamic phases were scanned, which were the hepatic arterial phase (15 s), portal venous phase (50 s), substantial period phase (90 s), and delayed phase (180 s); and (3) breath-hold diffusion-weighted echo-planar sequence (field of view, 400–343 mm; matrix size,  $116 \times 97$ ; repetition time/TE, 2500/64 ms; section thickness, 7 mm; intersection gap, 1 mm;  $b$  value = 0 and 800  $\text{s}/\text{mm}^2$ ).

**Fig. 1** Flowchart of study enrollment



## TACE treatment

All enrolled patients were successfully treated with TACE, including conventional TACE (cTACE) and drug-eluting bead TACE (DEB-TACE). It depends on the physicians to choose cTACE or DEB-TACE based upon the liver function of the patients, the size and number of tumors, whether diffuse or discrete, and their location in the liver. The TACE method recommended by the physician is approved by the patients. All therapeutic procedures were performed according to the current practice guidelines [20] and conducted by interventional radiologists with more than 10 years of clinical experience to ensure the standardization of the treatment process, and successful embolization was determined when no contrast staining in the tumor was identified on postembolization angiography.

For cTACE, lipiodol (Guerbet), gelatin sponge particles, and polyvinyl alcohol were used as embolic agents. The 2.7-Fr microcatheter (Progreat; Terumo) was applied to inject the embolic agents in the hepatic arterial vasculature under the monitoring of digital subtraction angiography (DSA; AlluraClarity FD 20, Philips). All patients were admitted after the cTACE procedures for post-procedure supportive treatment, and routine management was conducted, including hydration, antiemetics, pain control, and monitoring liver function changes.

For DEB-TACE, CalliSpheres® Beads (CB; Jiangsu Hengrui Medicine Co., Ltd.) with a diameter of 100–300  $\mu\text{m}$  were used as carriers and loaded with 60–80 mg epirubicin, pirubicin, or doxorubicin. The treatment process of TACE was similar to that of cTACE, with complete blockage of the tumor-supplying artery as the treatment endpoint.

## Evaluation of TACE response based on the modified Response Evaluation Criteria in Solid Tumors (mRECIST) criterion

We evaluated the modified Response Evaluation Criteria in Solid Tumors (mRECIST)-based tumor response in patients who underwent TACE treatment by postoperative MRI within 3–4 months. Briefly, the corresponding response of mRECIST [21] included (1) complete response (CR): complete disappearance of the tumor; (2) partial response (PR): a minimum 30% decrease in the sum of diameters of viable target lesions (enhancement in the arterial phase); (3) progressive disease (PD): at least 20% increase in the sum of the diameters of viable (enhancing) target lesions; and (4) stable disease (SD): neither PR nor PD. In the present study, the patients were divided into two groups: the TACE response (TR) group (CR and PR patients) and the non-TACE response

(nTR) group (PD and SD patients). Representative MR images for nTR and TR patients are shown in Fig. 2.

The TACE response of patients in this study was determined by two experienced radiologists based on the follow-up MR images. Of the 99 enrolled patients, 46 patients were assigned to the nTR group and 53 patients were assigned to the TR group. Then, the patients were randomly divided into a training cohort (69 patients; nTR = 32, TR = 37) and a validation cohort (30 patients; nTR = 14, TR = 16) by setting seed points.

### Texture feature extraction

All preoperative T2-weighted images were imported into ITK-SNAP ([www.itk-snap.org](http://www.itk-snap.org)) to delineate the volume of interest (VOI) of tumor areas, which was independently conducted by two radiologists with more than 15 years of experience in clinical diagnosis to secure the reproducibility of the intra-observer and inter-observer segmentation.

Then, the quantitative features of VOIs were calculated by Artificial Intelligence Kit software (A.K. software; GE Healthcare), and a total of 396 radiomics features were extracted for further analysis, which were divided into five categories, including histogram, form factors, gray-level size zone matrix

(GLSZM), gray-level co-occurrence matrix (GLCM), and run-length matrix (RLM).

### Selection of radiomics features and construction of the radiomics signature

All extracted radiomics features were further processed for dimension reduction, and the Z-score method was first used to standardize the features before feature dimension reduction, which could remove the unit limits on the data of each feature. Then, the abnormal values were replaced with the median of the parameter in all cases, and the training cohort was used to build the radiomics model, which was further verified by the validation cohort. Feature selection was performed with the least absolute shrinkage and selection operator (LASSO) logistic regression algorithm, and finally, the highly correlated features were screened. Then, the radiomics score (Rad-score) for each patient was calculated by using a linear combination of the cluster of the selected features, which were weighted by their corresponding LASSO coefficients. The predictive accuracy of the radiomics signature was quantified by the area under the receiver operating characteristic curve (AUC) in both the training and validation cohorts.

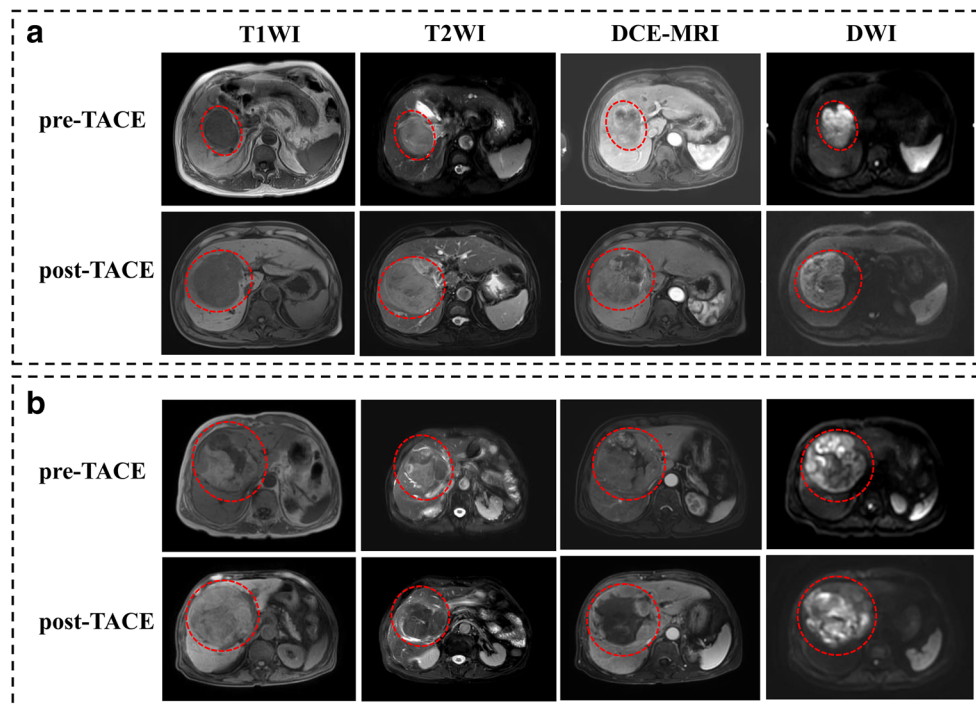


**Fig. 2** Representative MR images for nTR and TR of HCC patients according to mRECIST criterion. **a** A 73-year-old male HCC patient with a lesion diameter of 69.82 mm underwent MR scanning 1 week before TACE, followed by MR scanning 42 days after TACE. T1WI, T2WI, DCE-MRI, and DWI images were collected, and the results showed that the tumor presented with nTR, with the lesion diameter increasing to 98.79 mm. **b** An 80-year-old male HCC patient, with a lesion diameter

of 69.20 mm. MR scanning was performed 1 week before TACE, followed by MR scanning 42 days after TACE, and the results showed the lesion presented with partial response (TR), with the lesion diameter decreasing to 64.32 mm and 85% necrosis. MR, magnetic resonance; TACE, transcatheter arterial chemoembolization; TR, TACE response; nTR, non-TACE response; HCC, hepatocellular carcinoma; mRECIST, modified Response Evaluation Criteria in Solid Tumors

Furthermore, to improve the prediction performance of the current Rad-score-based model, we further introduced the clinical indicators that were highly correlated with TACE response into our predictive model. Univariate analysis and multivariate analysis were applied to select the highly correlated indicators for each potential clinical indicator, and then combined with the Rad-score to construct a radiomics nomogram as the predictive model for TACE response. The receiver operating characteristic (ROC) curves were plotted to evaluate the predictive ability of the model. Furthermore, to assess the calibration and clinical utility of the nomogram, calibration curves and decision curves were developed. Finally, the model was validated in the validation cohort by using the formula constructed in the training cohort to calculate the AUC and develop the calibration curve.

### Intra-observer and inter-observer agreement

The intra-observer agreement and inter-observer agreement of feature extraction were evaluated by correlation coefficients (ICCs). To compute the intra-observer ICC, 40 T2W MR images were selected randomly and segmented twice in 1 month by reader A. To compute the inter-observer ICC, the selected images were segmented by two radiologists independently (reader A and reader B). Segmentation was performed to further obtain independent feature extraction to compute the intra-observer and inter-observer ICCs. When the ICC was greater than 0.75, it was considered good agreement, and the remaining segmentation was performed by reader A.

### Statistical analysis

All quantitative features were analyzed with R software (version 3.6.1). The differences in clinical indicators between the training and validation cohorts were assessed by using the Kolmogorov-Smirnov test, and Student's *t* test. The LASSO logistic regression model was performed using the “glmnet” package. The “pROC” package was used to plot ROC curves. The nomogram and calibration curve were depicted using the “rms” package. The correlation analysis between radiomics features was performed using the “pheatmap” package. The clinical utility of our model was evaluated by a decision curve, which was plotted using the “rmda” package [22]. The reported statistical significance levels were all two-sided, with statistical significance set at 0.05.

## Results

### Clinical features of patients and logistic regression analysis of factors related to TR

In this study, a total of 99 patients who received TACE treatment with different responsiveness levels were enrolled according to the inclusion and exclusion criteria. The baseline

characteristics of the nTR and TR patients are listed in Table 1. Among them, 50 patients received cTACE treatment, 49 patients received DEB-TACE treatment, and 53 patients had responding, but 46 patients had no responding. Forty males (87.0%) and 6 females (13.0%) were included in the nTR group, with a median age of 54.5 years, and 44 males (83.0%) and 9 females (17.0%) were included in the TR group, with a median age of 65 years. At the initial diagnosis, the median diameter of the tumor was 5.3 cm (range from 3.60 to 9.15 cm) and 5.1 cm (range from 2.825 to 8.175 cm) in the nTR and TR groups, respectively. No significant difference was found in terms of sex, hepatitis B surface antigen (HBsAg), total bilirubin, carcinoembryonic antigen (CEA), tumor diameter, or therapy method between the nTR and TR groups ( $p > 0.05$ ). Meanwhile, there were large differences between the two groups in Child-Pugh class ( $p = 0.009$ ), BCLC stage ( $p = 0.007$ ), and alpha-fetoprotein (AFP) level ( $p = 0.003$ ).

Multivariate logistic regression analysis revealed that the Child-Pugh class, BCLC stage, and AFP level could be used as predictive factors for TR, as shown in Table 1. The ORs for Child-Pugh class, BCLC stage, and AFP level were 2.846 (95% CI: 1.054–7.680;  $p = 0.039$ ), 2.904 (95% CI: 1.136–7.426;  $p = 0.036$ ), and 1.001 (95% CI: 1.000–1.002;  $p = 0.006$ ), respectively. All the factors remained significant in both univariate analysis and multivariate analysis.

### Intra-observer and inter-observer reproducibility of radiomics feature extraction

There was no statistically significant difference between the measurements of the two readers for each selected feature, with  $p$  values ranging from 0.712 to 0.861. The intra-observer ICC calculated based on two measurements obtained by reader A ranged from 0.821 to 0.946. The inter-observer agreement between the two readers ranged from 0.767 to 0.910. The results indicated favorable intra- and inter-observer feature extraction reproducibility. Finally, all outcomes were based on the measurement of reader A.

### Radiomics model based on the Rad-score and clinical predictive factors

The workflow of radiomics in this study is shown in Fig. 3 and Figure S1. Ultimately, six features that were most strongly associated with the TR were selected by LASSO logistic regression: variance, InverseDifferenceMoment\_angle90\_offset7, LongRunEmphasis\_angle90\_offset7, ShortRunEmphasis\_AllDirection\_offset4\_SD, ShortRunEmphasis\_angle135\_offset1, and HighIntensityLargeAreaEmphasis (Table 2 and Figure S1C). The ROC curves for the selected features are presented in Fig. 4a and b, and the corresponding AUC, sensitivity, and specificity are shown in Table 2.

**Table 1** Baseline characteristics of the patients in the nTR and TR groups

Variables	Univariate analysis			Multivariate analysis	
	nTR ( <i>n</i> = 46)	TR ( <i>n</i> = 53)	<i>p</i> value	OR (95% CI)	<i>p</i> value
Age	54.5 (50, 65.25)	65.0 (50.0, 71.5)	0.054		
Sex			0.586		
Male	40 (87.0%)	44 (83.0%)			
Female	6 (13.0%)	9 (17.0%)			
Child-Pugh			0.009	2.846 (1.054, 7.680)	0.039
A	23 (50.0%)	40 (75.5%)			
B	23 (50.0%)	13 (24.5%)			
BCLC stage			0.007	2.904 (1.136, 7.426)	0.026
B	18 (39.1%)	35 (66.0%)			
C	28 (60.9%)	18 (34.0%)			
HBsAg			0.492		
Positive	36 (81.8%)	38 (76.0%)			
Negative	8 (18.2%)	12 (24.0%)			
AFP (ng/ml)	134.1 (18.9, 2000)	21.7 (5.2, 75.275)	0.003	1.001 (1.000, 1.002)	0.006
TBIL (μmol/L)	19.15 (11.05, 27.475)	15.7 (11.7, 19.7)	0.059		
CEA (U/ml)	2.9 (2.0, 4.25)	3.0 (2.1, 4.5)	0.911		
TD (cm)	5.3 (3.6, 9.15)	5.1 (2.825, 8.175)	0.458		
Therapy method			0.476		
cTACE	25 (54.3%)	25 (47.2%)			
DEB-TACE	21 (45.7%)	28 (52.8%)			

Skewness and kurtosis test was used to test the normality of continuous variables. Independent sample *t* test was used to compare continuous variables with normal distribution. Mann-Whitney *U*-test was used to compare continuous variables with abnormal distribution. Chi-square test was used for the comparisons of categorical variables. *p* value < 0.05 indicates a significant difference in patients' characteristics between the nTR and TR patients

TACE, transcatheter arterial chemoembolization; nTR, non-TACE response; TR, TACE response; Child-Pugh, Child-Pugh-Turcotte score; BCLC, Barcelona Clinic Liver Cancer; HBsAg, hepatitis B surface antigen; AFP, alpha-fetoprotein; TBIL, total bilirubin; CEA, carcinoembryonic antigen; TD, tumor diameter; cTACE, conventional TACE; DEB-TACE, drug-eluting bead TACE

Then, all six selected features were combined to generate the Rad-score for each case to construct a prediction model for TR. The model showed excellent predictive performance in the training and validation cohorts (Fig. 4c, d). In the training cohort, the AUC of the prediction model was 0.812 (95% CI: 0.711 to 0.914), and the specificity and sensitivity were 0.676 and 0.844, respectively. In the validation cohort, the AUC, specificity, and sensitivity were 0.866 (95% CI: 0.739 to 0.993), 0.812, and 0.786, respectively.

To improve the prediction efficiency of the above model based on the Rad-score, we further integrated the screened clinical indicators (Child-Pugh class, BCLC stage, and AFP level) into the prediction model to form a novel model, and the performance of the model was improved significantly (Fig. 5 and Table 3). The AUC of the training cohort was 0.861 (95% CI: 0.774 to 0.949), and the specificity and sensitivity were as high as 0.811 and 0.844, respectively. The AUC of the validation cohort was 0.884 (95% CI: 0.764 to 1.000), and the specificity and sensitivity were 0.75 and 1.00, respectively.

### Construction of the predictive nomogram

A radiomics nomogram was constructed on the basis of the above novel prediction model, which effectively

incorporated both the Rad-score and selected clinical predictors (Fig. 6a). The calibration plot also indicated good agreement between the nomogram prediction and actual observation for patients in both the training and validation cohorts (Fig. 6b, c).

### Clinical utility of the predictive nomogram

The decision curve analysis for the radiomics nomogram is presented in Figure S2. The decision curve showed that if the threshold probability of a patient was > 7%, using the radiomics nomogram to predict nTR adds more benefit than either the treat-none scheme or the treat-all-patients scheme. Within this range, on the basis of the above radiomics nomogram, the net benefit was comparable, with several overlaps.

### Discussion

TACE is a widely used locoregional palliative interventional therapy, and it plays a pivotal role in the management of HCC patients due to the blockage of the blood-supplying artery of tumors, which could cause extensive necrosis and inhibit tumor

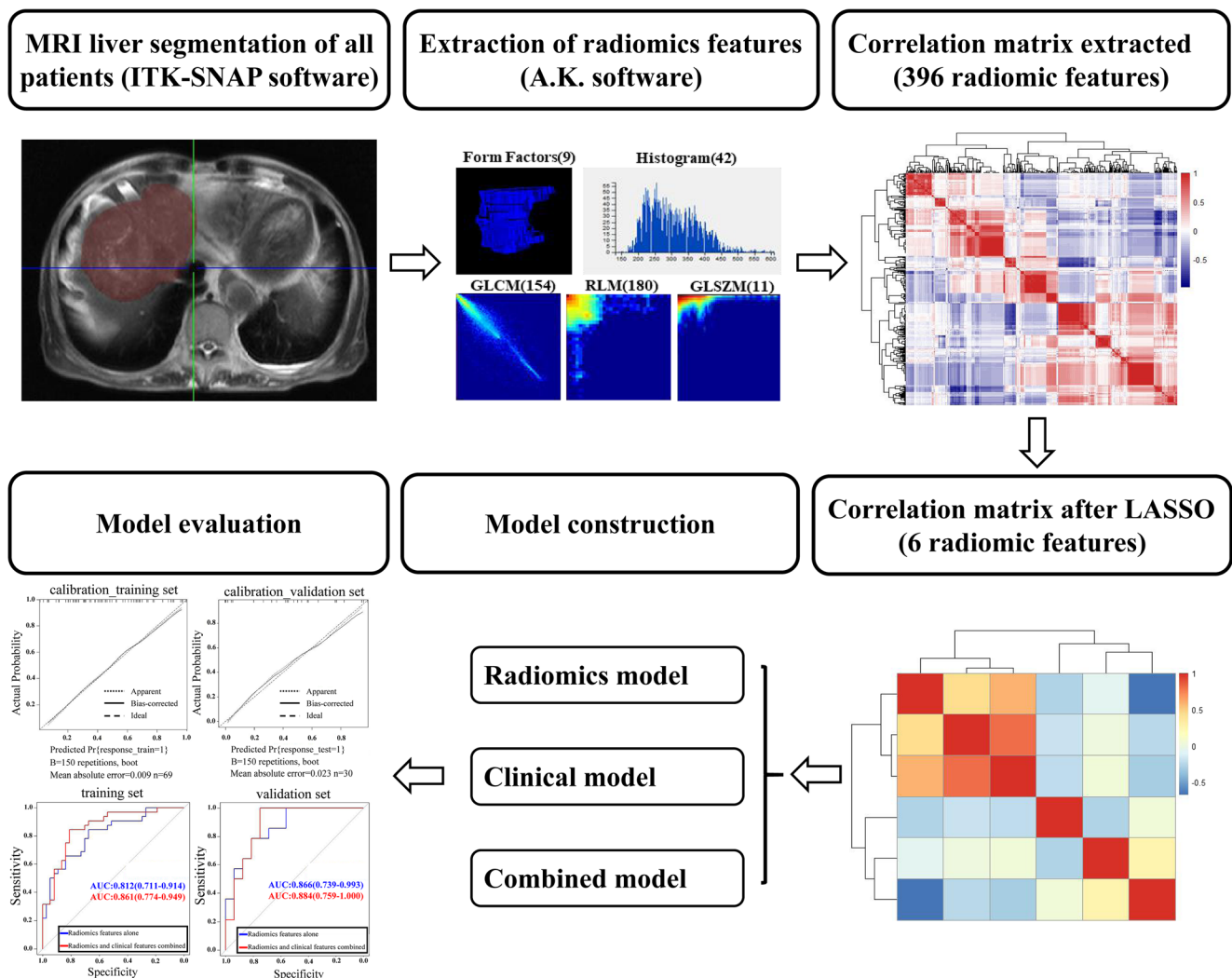


**Fig. 3** Flowchart of the study. The flowchart shows the overall operational process. First, VOIs were manually depicted based on raw MR imaging with ITK-SNAP software. Second, 396 features were extracted from the VOI of each patient by using the A.K. software, which had high correlation, as shown by the correlation matrix. Third, the LASSO method was applied for data dimension reduction, feature

selection, and model construction. Finally, the performance of the radiomics features model, clinical features model, and the combined model were evaluated by the AUCs of the ROC curves, calibration curves, and decision curves. VOI, volume of interest; MR, magnetic resonance; LASSO, least absolute shrinkage and selection operator; AUC, area under the curve; ROC, receiver operating characteristic

**Table 2** Predictive performance of each feature selected by LASSO in the training and validation cohorts

Category	Feature selected	Coefficient	AUC		Sensitivity		Specificity	
			Training	Validation	Training	Validation	Training	Validation
GLSZM	Variance	-0.4574	0.613	0.728	93.8%	57.1%	29.7%	93.8%
GLCM	InverseDifferenceMoment_angle90_offset7	0.3763	0.610	0.522	37.5%	50.0%	83.8%	75.0%
RLM	LongRunEmphasis_angle90_offset7	0.9905	0.761	0.688	65.6%	100%	81.1%	43.8%
RLM	ShortRunEmphasis_AllDirection_offset4_SD	-0.9054	0.612	0.661	43.8%	42.9%	81.1%	100%
RLM	ShortRunEmphasis_angle135_offset1	-0.4763	0.694	0.701	62.5%	92.9%	73.0%	56.2%
Histogram	HighIntensityLargeAreaEmphasis	-0.0684	0.687	0.812	53.1%	64.3%	78.4%	93.8%
	Constant	-0.1068						

LASSO, least absolute shrinkage and selection operator; AUC, the area under the operating characteristic curve; GLSZM, gray-level size zone matrix; GLCM, gray-level co-occurrence matrix; RLM, run-length matrix

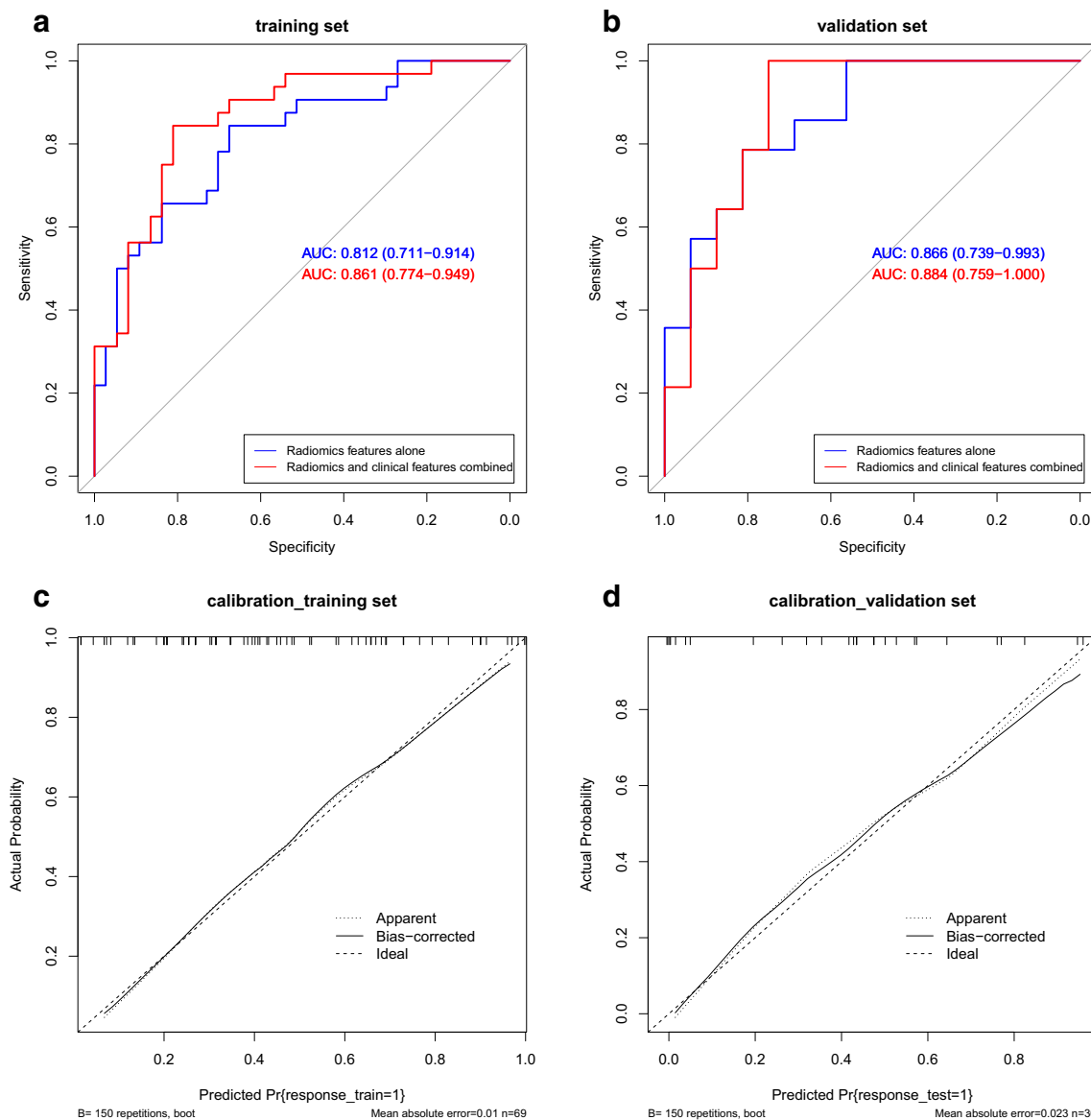


**Fig. 4** The predictive performance of each of the selected features and the Rad-score-based model. **a, b** ROC curves of each of the selected imaging features in the training and validation cohorts, respectively. **c, d** The predictive performance of the Rad-score-based model, as presented by

ROC curves in the training cohort (AUC = 0.812, 95% CI: 0.711 to 0.914) and validation cohort (AUC = 0.866, 95% CI: 0.739 to 0.993). ROC, receiver operating characteristic; AUC, area under the curve; 95% CI, 95% confidence interval

progression [23]. However, the clinical response of HCC patients to TACE tends to present large individual differences [8, 24]. Therefore, it is particularly important to accurately assess the tumor response before TACE, which is also essential for the further management of HCC. The present study developed and validated a novel predictive, radiomics signature and clinical predictor-based radiomics nomogram for predicting the responsiveness of TACE candidates with HCC. The model could successfully stratify patients into nTR and TR patients according to their pre-TACE Rad-scores and clinical characteristics.

In the present study, radiomics technology was applied to extract texture features in T2WI of HCC patients, and 396

candidate radiomics features were applied for further study. Among these 396 radiomics features, there are 42 histogram-based features, 9 form factor-based features, 11 GLSZM-based features, 180 RLM-based features, and 154 GLCM-based features. The histogram-based features were calculated using the intensity (HU) distribution of a given ROI and reflect the intensity information of tumors [25]. The form factor-based parameters can describe the three-dimensional size and shape of the tumor region. The GLSZM-based features compute the number of times a pixel with a specific gray-level occurs with another pixel with a gray value jointly. It represents the joint probability of specific pixels having certain gray-level values [26]. The

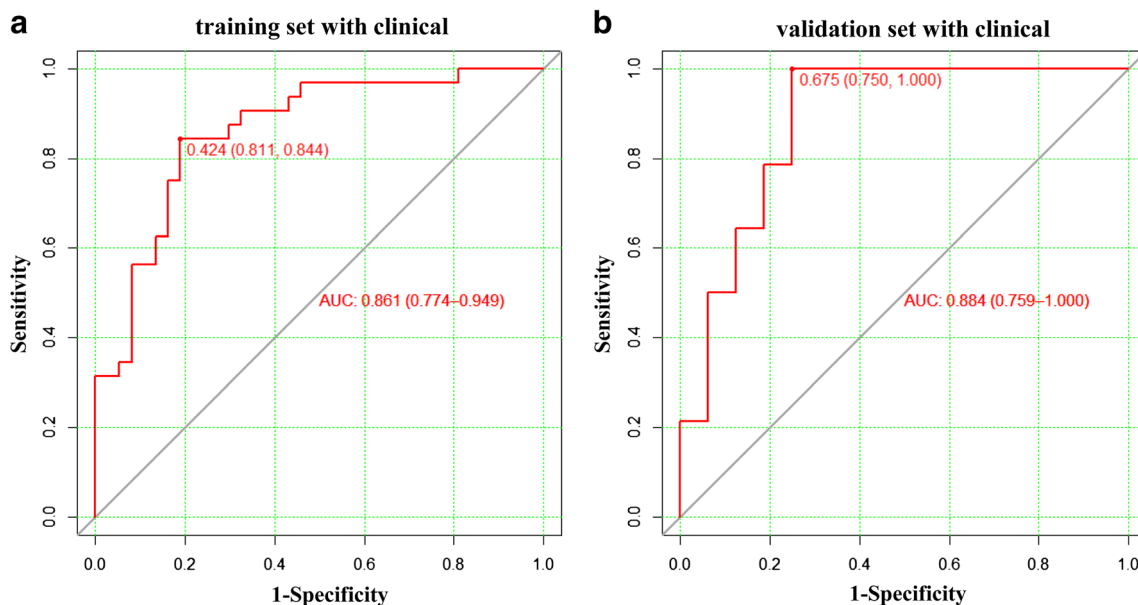


**Fig. 5** The predictive performance of the model based on the Rad-score and clinical indicators. **a, b** ROC curves of the combined model in the

training and validation cohorts, respectively. ROC, receiver operating characteristic

RLM-based features were defined as the number of runs with pixels of different gray levels and run lengths for a given direction such as those defined by GLCM [27].

In our study, the potential 396 candidate radiomics features were finally reduced to six potential predictors by shrinking the regression coefficients with the LASSO method for further integration to form the Rad-score, which contains effective biological information and could reflect the heterogeneity of the tumor [18]. Several previous studies have demonstrated that the Rad-score could effectively predict the prognosis of patients due to its high correlation with tumor biological characteristics [28, 29]. For TACE response, a recent study showed that the computed tomography-based radiomics signature was closely associated with the early recurrence of HCC after TACE [30]. These preliminary studies have further confirmed that the texture feature-based radiomics method is feasible for predicting TACE responsiveness.

The BCLC staging system and Child-Pugh class have been endorsed and recommended by multiple guidelines for prognosis and treatment stratification of HCC patients [31, 32], and plenty of studies have also demonstrated that BCLC stage and Child-Pugh class could be used as important

indicators for the prognosis of HCC [33–35]. In addition, some studies have focused on the relationship between laboratory indicators (such as AFP, CEA, or HBsAg) and the prognosis of HCC [36–38]. In our study, univariate and multivariate analyses were also used to select the clinical predictors. The obtained results showed that BCLC stage, Child-Pugh class, and AFP level were highly correlated with TR and could be used as independent predictors. Then, the above three clinical predictors were combined with the radiomics signature to construct a novel TR prediction nomogram, which could effectively improve the predictive performance of the model based on the Rad-score.

The constructed novel TR prediction nomogram was further evaluated by a decision curve to clarify the clinical utility, which could offer insight into clinical outcomes on the basis of threshold probability, from which the net benefit could be derived (net benefit is defined as the differential value of true positives proportion and false positives proportion, weighted by the relative harm of false positive and false negative results) [39, 40]. The results showed that if the threshold probability of a patient is > 7%, using the radiomics nomogram in this study to predict poor tumor response of patients treated with TACE adds more

**Table 3** Comparison of the predictive performance for tumor response of each model in the training and validation cohorts

Models	Training cohort			Validation cohort		
	AUC	Sensitivity	Specificity	AUC	Sensitivity	Specificity
Radiomics model	0.812	84.4%	67.6%	0.866	78.6%	81.2%
Clinical model	0.733	62.5%	73.0%	0.667	42.9%	93.8%
Combined model	0.861	84.4%	81.1%	0.884	100%	68.8%

AUC, the area under the operating characteristic curve

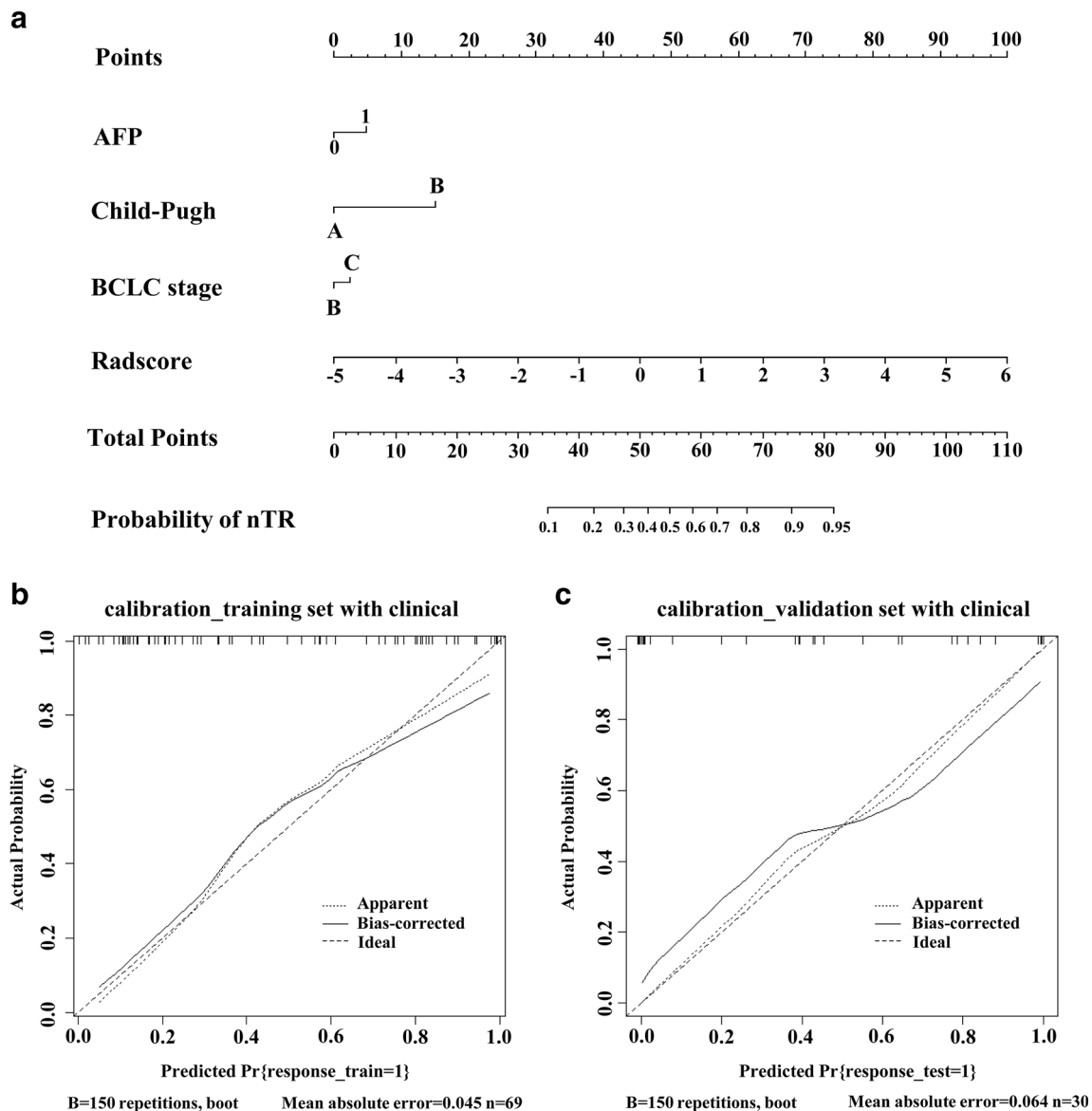


**Fig. 6** The nomogram and calibration curves of the model based on the radiomics signature and clinical predictors. **a** The radiomics nomogram integrated the radiomics signature with the AFP level, Child-Pugh class, and BCLC stage in the training cohort. The probability value of each HCC patient with nTR is marked on each axis. **b, c** The calibration curves between the nomogram prediction and actual observation for nTR and TR patients in the training and validation cohorts, respectively. The diagonal

dotted line represents an ideal evaluation, while the solid lines and dashed lines represent the performance of the corrected and apparent bias, respectively. The closer the fit is to the diagonal dotted line, the better the evaluation. AFP, alpha-fetoprotein; BCLC, Barcelona Clinic Liver Cancer; HCC, hepatocellular carcinoma; TACE, transcatheter arterial chemoembolization; TR, TACE response; nTR, non-TACE response

benefit than either the treat-all-patients scheme or the treat-none scheme. The present novel nomogram provides an important quantitative indicator and reference for the decision-making and management of treatment regimens for clinical HCC patients.

The GIDEON study showed that cTACE and DEB-TACE comprise 74% and 16% of TACE procedures, respectively [41]. In clinic, the physicians chose cTACE or DEB-TACE for the treatment of HCC patients based upon the liver function of the patients, the number and size of tumors, whether discrete or diffuse, and their location in the livers. In order to obtain a

universally applicable prognostic model for TACE, patients receiving cTACE or DEB-TACE were all enrolled in this study. The results showed that the TACE techniques were not an independent predictor for tumor response. The result is consistent with a recent study, which shows that there has been no statistical difference in efficacy (tumor response and overall survival) between cTACE and DEB-TACE [42]. Doxorubicin, epirubicin, and pirubicin are the most commonly used anticancer drugs in TACE treatment. A randomized controlled trial showed that there is no significant difference in survival among doxorubicin,

cisplatin, and epirubicin [43]. The choice of the anticancer agent and the administered dose are recommended by the interventional radiologists based on the condition of the patients [44].

However, there are several limitations in our study. First, selection bias was inevitable because the current study was a single-center, retrospective study. Second, the sample size was relatively small, and external validation and larger datasets are needed to validate and refine our results. In the future, large samples, multi-center cohorts, and multimodal research should be conducted to validate the prognostic significance of this radiomics signature.

In conclusion, radiomics provides a novel method to extract potentially important data from clinical imaging that can identify different clusters. The constructed novel TR prediction nomogram is a novel, noninvasive, efficient, and feasible method for the prediction of clinical TACE responsiveness in HCC patients. The quantitative nomogram prediction model based on the Rad-score and clinical predictors may serve as an alternative method for precision medicine and provide highly informative data for making clinical management decisions. Furthermore, the present study provides new strategies for more precise and personalized management of HCC patients, which could also be extended to other types of treatment.

**Supplementary Information** The online version contains supplementary material available at <https://doi.org/10.1007/s00330-021-07910-0>.

**Funding** This study was supported by the National Key Research and Development Projects Intergovernmental Cooperation in Science and Technology of China (2018YFE0126900 to JS. Ji), National Natural Science Foundation of China (81901852 to MJ. Chen, 81901848 to JJ. Song), Zhejiang Medical and Health Science Project (2018KY933 to JF. Tu, 2020ZH087 to XH. Ying), Natural Science Foundation of Zhejiang Province (LGF21H180002 to CL. Kong, LQ20H160055 to SJ. Fang), and The Key Research and Development Program of Lishui City (2019ZDYF17 to JS. Ji).

## Declarations

**Guarantor** The scientific guarantor of this publication is Jiansong Ji.

**Conflict of interest** The authors of this manuscript declare no relationships with any companies whose products or services may be related to the subject matter of the article.

**Statistics and biometry** No complex statistical methods were necessary for this paper.

**Informed consent** Written informed consent was waived by the Institutional Review Board.

**Ethical approval** Institutional Review Board approval was obtained.

## Methodology

- retrospective
- diagnostic or prognostic study
- performed at one institution

**Open Access** This article is licensed under a Creative Commons Attribution 4.0 International License, which permits use, sharing, adaptation, distribution and reproduction in any medium or format, as long as you give appropriate credit to the original author(s) and the source, provide a link to the Creative Commons licence, and indicate if changes were made. The images or other third party material in this article are included in the article's Creative Commons licence, unless indicated otherwise in a credit line to the material. If material is not included in the article's Creative Commons licence and your intended use is not permitted by statutory regulation or exceeds the permitted use, you will need to obtain permission directly from the copyright holder. To view a copy of this licence, visit <http://creativecommons.org/licenses/by/4.0/>.

## References

1. El-Serag HB, Rudolph KL (2007) Hepatocellular carcinoma: Epidemiology and molecular carcinogenesis. *Gastroenterology* 132:2557–2576
2. Torre LA, Bray F, Siegel RL, Ferlay J, Lortet-Tieulent J, Jemal A (2015) Global cancer statistics, 2012. *CA Cancer J Clin* 65:87–108
3. Sciarra A, Di Tommaso L, Nakano M et al (2016) Morphophenotypic changes in human multistep hepatocarcinogenesis with translational implications. *J Hepatol* 64:87–93
4. Pinna AD, Yang T, Mazzaferro V et al (2018) Liver transplantation and hepatic resection can achieve cure for hepatocellular carcinoma. *Ann Surg* 268:868–875
5. Huang F, Gong H, Xiong Z (2018) The safety and efficacy of raltitrexed combined with oxaliplatin in TACE treatment for BCLC B/C hepatocellular carcinomas. *Chin J Radiol* 27:76–79
6. Goumar C, Komatsu S, Brustia R, Fartoux L, Soubrane O, Scatton O (2017) Technical feasibility and safety of laparoscopic right hepatectomy for hepatocellular carcinoma following sequential TACE-PVE: A comparative study. *Surg Endosc* 31:2340–2349
7. Lencioni R, Llovet JM, Han G et al (2016) Sorafenib or placebo plus TACE with doxorubicin-eluting beads for intermediate stage HCC: The SPACE trial. *J Hepatol* 64:1090–1098
8. Wang JH, Zhong XP, Zhang YF et al (2017) Cezanne predicts progression and adjuvant TACE response in hepatocellular carcinoma. *Cell Death Dis* 8:e3043
9. Tsurusaki M, Murakami T (2015) Surgical and locoregional therapy of HCC: TACE. *Liver Cancer* 4:165–175
10. Kucukay F, Badem S, Karan A et al (2015) A single-center retrospective comparison of doxorubicin-loaded HepaSphere transarterial chemoembolization with conventional transarterial chemoembolization for patients with unresectable hepatocellular carcinoma. *J Vasc Interv Radiol* 26:1622–1629
11. Takaki S, Sakaguchi H, Anai H et al (2012) Long-term outcome of transcatheter subsegmental and segmental arterial chemoembolization using lipiodol for hepatocellular carcinoma. *Cardiovasc Intervent Radiol* 35:544–554
12. Jiang BG, Wang N, Huang J et al (2017) Tumor SOCS3 methylation status predicts the treatment response to TACE and prognosis in HCC patients. *Oncotarget* 8:28621–28627
13. Vesselle G, Quirier-Leleu C, Velasco S et al (2016) Predictive factors for complete response of chemoembolization with drug-

- eluting beads (DEB-TACE) for hepatocellular carcinoma. *Eur Radiol* 26:1640–1648
14. Kim SY, An J, Lim YS et al (2017) MRI with liver-specific contrast for surveillance of patients with cirrhosis at high risk of hepatocellular carcinoma. *JAMA Oncol* 3:456–463
  15. Zhang B, Tian J, Dong D et al (2017) Radiomics features of multiparametric MRI as novel prognostic factors in advanced nasopharyngeal carcinoma. *Clin Cancer Res* 23:4259–4269
  16. Zinn PO, Singh SK, Aikaterini K et al (2016) Clinically applicable and biologically validated MRI radiomic test method predicts glioblastoma genomic landscape and survival. *Neurosurgery* 63:156–157
  17. Li H, Zhu Y, Burnside ES et al (2016) MR imaging radiomics signatures for predicting the risk of breast cancer recurrence as given by research versions of MammaPrint, oncotype DX, and PAM50 gene assays. *Radiology* 281:382–391
  18. Ganeshan B, Miles KA (2013) Quantifying tumour heterogeneity with CT. *Cancer Imaging* 13:140–149
  19. Kim J, Choi SJ, Lee SH, Lee HY, Park H (2018) Predicting survival using pretreatment CT for patients with hepatocellular carcinoma treated with transarterial chemoembolization: Comparison of models using radiomics. *AJR Am J Roentgenol* 211:1026–1034
  20. Gaba RC, Lokken RP, Hickey RM et al (2017) Quality improvement guidelines for transarterial chemoembolization and embolization of hepatic malignancy. *J Vasc Interv Radiol* 28:1210–1223 e1213
  21. Lencioni R, Montal R, Torres F et al (2017) Objective response by mRECIST as a predictor and potential surrogate end-point of overall survival in advanced HCC. *J Hepatol* 66:1166–1172
  22. Vickers AJ, Cronin AM, Elkin EB, Gonen M (2008) Extensions to decision curve analysis, a novel method for evaluating diagnostic tests, prediction models and molecular markers. *BMC Med Inform Decis Mak* 8:53
  23. Lencioni R, Llovet JM, Han G et al (2012) Sorafenib or placebo in combination with transarterial chemoembolization (TACE) with doxorubicin-eluting beads (DEBDOX) for intermediate-stage hepatocellular carcinoma (HCC): Phase II, randomized, double-blind SPACE trial. *J Clin Oncol* 30:LBA154
  24. Wang W, Zhao Y, Bai W, Han G (2015) Response assessment for HCC patients treated with repeated TACE: The optimal time-point is still an open issue. *J Hepatol* 63:1530–1531
  25. Lee SW, Park H, Lee HY et al (2018) Deciphering clinicoradiologic phenotype for thymidylate synthase expression status in patients with advanced lung adenocarcinoma using a radiomics approach. *Sci Rep* 8:8968
  26. Feng Q, Chen Y, Liao Z et al (2018) Corpus callosum radiomics-based classification model in Alzheimer's Disease: A case-control study. *Front Neurol* 9:618
  27. Yang D, Rao G, Martinez J, Veeraraghavan A, Rao A (2015) Evaluation of tumor-derived MRI-texture features for discrimination of molecular subtypes and prediction of 12-month survival status in glioblastoma. *Med Phys* 42:6725–6735
  28. Segal E, Sirlin CB, Ooi C et al (2007) Decoding global gene expression programs in liver cancer by noninvasive imaging. *Nat Biotechnol* 25:675–680
  29. Kuo MD, Gollub J, Sirlin CB, Ooi C, Chen X (2007) Radiogenomic analysis to identify imaging phenotypes associated with drug response gene expression programs in hepatocellular carcinoma. *J Vasc Interv Radiol* 18:821–831
  30. Ning P, Gao F, Hai J et al (2020) Application of CT radiomics in prediction of early recurrence in hepatocellular carcinoma. *Abdom Radiol (NY)* 45:64–72
  31. Duseja A (2014) Staging of hepatocellular carcinoma. *J Clin Exp Hepatol* 4:S74–S79
  32. Piscaglia F, Terzi E, Cucchetti A et al (2013) Treatment of hepatocellular carcinoma in Child-Pugh B patients. *Dig Liver Dis* 45:852–858
  33. Nakagawa S, Hayashi H, Nitta H et al (2015) Scoring system based on tumor markers and Child-Pugh classification for HCC patients who underwent liver resection. *Anticancer Res* 35:2157–2163
  34. Zhao WH, Ma ZM, Zhou XR, Feng YZ, Fang BS (2002) Prediction of recurrence and prognosis in patients with hepatocellular carcinoma after resection by use of CLIP score. *World J Gastroenterol* 8:237–242
  35. Tateishi R, Shiina S, Yoshida H et al (2006) Prediction of recurrence of hepatocellular carcinoma after curative ablation using three tumor markers. *Hepatology* 44:1518–1527
  36. Zheng BH, Liu LZ, Zhang ZZ et al (2018) Radiomics score: A potential prognostic imaging feature for postoperative survival of solitary HCC patients. *BMC Cancer* 18:1148
  37. Yuan C, Wang Z, Gu D et al (2019) Prediction early recurrence of hepatocellular carcinoma eligible for curative ablation using a radiomics nomogram. *Cancer Imaging* 19:21
  38. Jeong SO, Kim EB, Jeong SW et al (2017) Predictive factors for complete response and recurrence after transarterial chemoembolization in hepatocellular carcinoma. *Gut Liver* 11:409–416
  39. Collins GS, Reitsma JB, Altman DG, Moons KG (2015) Transparent reporting of a multivariable prediction model for individual prognosis or diagnosis (TRIPOD): The TRIPOD statement. *BMJ* 350:g7594
  40. Balachandran VP, Gonen M, Smith JJ, DeMatteo RP (2015) Nomograms in oncology: More than meets the eye. *Lancet Oncol* 16:e173–e180
  41. Geschwind JF, Kudo M, Marrero JA et al (2016) TACE treatment in patients with sorafenib-treated unresectable hepatocellular carcinoma in clinical practice: Final analysis of GIDEON. *Radiology* 279:630–640
  42. Raoul JL, Fomer A, Bolondi L, Cheung TT, Kloeckner R, de Baere T (2019) Updated use of TACE for hepatocellular carcinoma treatment: How and when to use it based on clinical evidence. *Cancer Treat Rev* 72:28–36
  43. Marelli L, Stigliano R, Triantos C et al (2007) Transarterial therapy for hepatocellular carcinoma: Which technique is more effective? A systematic review of cohort and randomized studies. *Cardiovasc Intervent Radiol* 30:6–25
  44. Wang YX, De Baere T, Idee JM, Ballet S (2015) Transcatheter embolization therapy in liver cancer: An update of clinical evidences. *Chin J Cancer Res* 27:96–121

**Publisher's note** Springer Nature remains neutral with regard to jurisdictional claims in published maps and institutional affiliations.